

Practical Concerns for Estimating Mixed Hidden Markov Models

1 Introduction

The circadian rhythm plays a major role in regulating human health. Disruption of the wake/sleep cycle is associated with a variety of negative health outcomes. For instance, the International Agency for Research on Cancer states that the chance of developing certain types of cancers is greatly increased when the circadian rhythm is disturbed. Sleep studies are the current gold standard to evaluate sleep, however they are resource intensive and thus can only focus on small groups at a time. Therefore, it is difficult to get population level data on the circadian rhythm.

The National Health Examination Survey (NHANES) is a collection of studies aiming to quantify the health of US civilians. Beginning in 1960, NHANES became a yearly study in 1999 where specific goals change year-to-year to focus on emerging issues. For two years in the mid 2010s, a representative sample for the US of 5,000 participants (for a total of 10,000) were given a wrist physical activity monitor (PAM) for 9 days. Among other metrics, these PAMs measured physical activity by the minute. This data offers a unique glimpse into the circadian rhythm for the US population as a whole.

The proliferation of personal PAMs offers an interesting insight into sleep health. Currently, a lengthy and expensive sleep study is needed in order to quantify the circadian rhythm. PAMs offer a possibility of gathering much larger amounts of data easily, however the data may not be as accurate. Although this is an exciting opportunity, there are two main challenges.

Firstly, PAMs measure activity not sleep. Although there is a clear connection between the two, the specific relationship is not immediately apparent. High activity periods most likely indicate an underlying wake state, however periods of inactivity may be hard to classify. For example, activity data may look similar for sedentary wake activities and sleep (e.g. watching TV may appear similar sleeping). Additionally, during periods of very low activity, measurements may be below the limit of detection (LoD). We propose to use an extension of a hidden Markov model (HMM) to capture this behavior. The observed data will be the activity measurements from the PAM and the hidden Markov state will be the unobserved wake/sleep status.

The second complication is that activity levels are heterogeneous across the population. Previously this

issue has been handled by either extending the Markov state space from wake and sleep to high activity wake, low activity wake, and sleep or by estimating the emission parameters independently for each person. In the first scenario, active people would spend a larger proportion of their wake time in the high activity wake state compared to the low activity wake state. This solution may cause more problems than it solves as there is no agreed upon cut off for what constitutes low/high activity. Additionally, this greatly increases the complexity of adding important covariates to the Markov transition matrix. Estimating a 3x3 transition matrix is much more difficult than a 2x2, causing feasibility issues when large amounts of data are used. For the second approach, although estimating the emission parameters independently allows a greater fit this too causes more issues than it solves. As the number of participants increases so too does the number of parameters. For datasets that do not have a large number of repeated measurements for each person this approach will not work. Lastly, it is not clear how this can be extrapolated to new data without re-estimation. Instead we propose a mixed HMM (MHMM) [1] with an individual level random effect for the activity data in the wake state. This allows people to have different levels of activity while keeping the interpretable and computation friendly two state structure.

This project focuses on practical concerns for estimation of a MHMM, with a focus on guidelines for estimating MHMMs. Specifically, we aim to answer whether a MHMM is necessary for state reconstruction, or if a HMM is sufficient. If a MHMM is necessary, we discuss how many support points are needed for the nonparametric density estimation for the emission distribution random effect (RE). Afterwards we apply a MHMM to the NHANES physical activity data.

2 Methods

2.1 Notation

Define the set $\{S_{i1}, \dots, S_{iT}\}$ as the states of a first order Markov chain (MC) corresponding to the wake/sleep cycle. If person i at time t is awake we let $S_{it} = 0$, otherwise if person i is asleep at time t then $S_{it} = 1$. To account for detection limit issues, let δ_{it} be 0 when the activity measurement is below the LoD and person i is asleep, and 1 otherwise. Therefore, we assume that when we observe a measurement below the LoD, the person must be in the sleep state. As this is a first order MC, it can be completely described by an initial probability, $P_j = P(S_{i1} = j)$, and a transition matrix where entry ij is equal to $P_{ij} = P(S_{it} = j | S_{it-1} = i)$. Define the set $\{a_{i1}, \dots, a_{iT}\}$ as the observed physical activity data from a PAM for patient i . For person i at time t , we refer to the probability of the activity measurement given the current wake/sleep state as the emission distribution. The activity measurement given the current wake/sleep status is independent of

all other MC states, or equivalently $P(a_{it}|S_{i1}, \dots, S_{iT}) = P(a_{it}|S_{it})$. Therefore the HMM can be completely described by the initial, transition, and emission probabilities.

To allow for covariates in the transition probabilities, we model the probability of changing states with the inverse-logit or expit function. We have $q(it)_{01} = \text{expit}(X_{it}\beta_0)$ and $q(it)_{10} = \text{expit}(X_{it}\beta_1)$ where X_{it} is a vector of covariates and β_j is the corresponding covariate parameters. This allows both fixed (e.g. race) and time varying (e.g. current time) covariates to influence the transition probabilities. In our simulation study we let $\beta_j = \{\beta_{j0}, \dots, \beta_{j4}\}$ and $X_{it} = \{1, x_{it1}, \dots, x_{it4}\}$, where x_{it1} and x_{it2} are fixed covariates equal to 1 if that covariate applies to person i . $x_{it3} = \cos(\frac{2\pi t}{96})$ and $x_{it4} = \sin(\frac{2\pi t}{96})$ are time varying to account for the cyclical nature of the circadian rhythm. Any first order harmonic function with a period of 96 can be estimated. A period of 96 was chosen as this is equivalent to modeling each day in 15 minute chunks.

We assume that the activity data given the underlying wake/sleep state is normally distributed. When person i is asleep, we assume a_{it} is drawn from a normal distribution centered at μ_1 with variance σ_1^2 . When person i is awake, we assume a_{it} is drawn from a normal distribution centered at $\mu_0 + u_i$ with variance σ_0^2 . u_i is an old-style random effect directly related to the mean wake activity of person i . We require that the distribution of u_i (H) has mean 0, but place no other restrictions on it. This assumption can be relaxed, however it facilitates easy comparison between simulations later on. To be clear, we do not necessarily assume that H is a normal distribution. There is little precedent on how activity is distributed across the US population and we did not want to automatically assume that it was normally distributed. Later on we will conduct a simulation study where H is varied. By including a RE in the model, we use the term mixed HMM (MHMM) to describe this model.

2.2 Estimation

Without applying any additional methods, the likelihood is written as equation 1. Inside of the square brackets, we evolve through the Markov chain for person i , multiplying the initial, transition, and emission probabilities. As we do not know the underlying MC state, it is not clear yet how to calculate these probabilities as the wake/sleep states are not observed. As u_i is a continuous individual level random effect, we must integrate over its support for each individual. This integral is complex and may require numerical methods to solve, increasing the computation required. The next two subsections will detail how to calculate this likelihood.

$$f(\mathbf{a}|\theta) = \prod_{i=1}^n \int_U \sum_{s_1 \dots s_T} \left[P(S_{i1}) = s_1 \prod_{t=2}^T P(S_{it} = s_t | S_{it-1} = s_{t-1}) \times \prod_{t=1}^T P(a_{it} | S_{it} = s_t, u_i)^{\delta_{it}} \right] dH(u_i) \quad (1)$$

2.2.1 Nonparametric Density Estimation (NPDE)

To simplify the integral (as well as allowing future computations with the forward-backward algorithm), we will estimate the RE distribution, H , with a discrete random variable, b_i . A small number of support points are chosen where the mass put on support point l is π_l . This can equivalently be written as $P(b_i = r_l) = \pi_l$ where r_l is support point l . Later on we will conduct a simulation study where the number of support points ranges from one to six. Conceptually, this can be thought of as estimating a discrete distribution using a histogram where each bar of the histogram is a support point and the mass put on each support point is the height of the bar. It is important to note that using one support point is equivalent to leaving out the RE and thus the MHMM reduces to a HMM. NPDE has been applied with success numerous times in various applications [2]. Using this approach we can write the likelihood as follows:

$$f(\mathbf{a}|\theta) = \prod_{i=1}^n \sum_{l=1}^L \sum_{s_1 \dots s_T} \left[P(S_{i1}) = s_1 \prod_{t=2}^T P(S_{it} = s_t | S_{it-1} = s_{t-1}) \times \prod_{t=1}^T P(a_{it} | S_{it} = s_t, b_i = r_l)^{\delta_{it}} \right] \pi_l \quad (2)$$

the change from equation 1 to 2 is that the integral over the support of U becomes a sum over the number of support points, L . Thus the time needed to compute this likelihood scales linearly with L . Increasing L increases estimation accuracy, however it comes at a computational price. L must be chosen before estimation, and there are no clear guidelines on how to do so.

2.2.2 EM Algorithm

The EM algorithm is an iterative technique to perform maximum likelihood estimation in the presence of latent variables [3]. Each iteration of the algorithm alternates between an expectation (E) and maximization (M) step, where the likelihood is guaranteed to increase between each iteration. Once the likelihood increase between iterations become sufficiently small, we consider the algorithm converged and stop. For the E step, we calculate the expected value of the full data log likelihood conditional on the observed data. We then maximize this expectation in the M step. The complete data likelihood can be written down as if we knew the latent variables that are required for estimation. It can be written as:

$$\begin{aligned}
f(\mathbf{a}, \mathbf{S}, \mathbf{b}|\theta) = & \prod_{i=1}^n \prod_{j=0}^1 P(S_{i1} = j)^{I(S_{i1}=j)} \times \\
& \prod_{i=1}^n \prod_{t=2}^T \prod_{k=0}^1 \prod_{j=0}^1 P(S_{it} = j | S_{it-1} = k)^{I(S_{it-1}=k, S_{it}=j)} \times \\
& \prod_{i=1}^n \prod_{l=1}^L \prod_{t=1}^T \prod_{j=0}^1 P(a_{it} | S_{it} = j, b_i = r_l)^{I(S_{it}=j, b_i=r_l)\delta_{it}} \\
& \prod_{i=1}^n \prod_{l=1}^L \pi_l^{I(b_i=r_l)}
\end{aligned} \tag{3}$$

where $I()$ is an indicator variable. We then take the expected value of the log of equation 3, conditioning on the observed data. The result is the expectation of the complete data log likelihood. Letting $p_j = P(S_{i1} = j)$, $p_{kj} = P(S_{it} = j | S_{it-1} = k)$, and $\pi_l = P(b_i = r_l)$ we can calculate the E step by calculating equation 4 using a modified version of the forward-backward algorithm, detailed in the next section.

$$\begin{aligned}
\ell = E[\log f(\mathbf{a}, \mathbf{S}, \mathbf{b}|\theta) | \mathbf{a}, \theta] = & \sum_{i=1}^n \sum_{j=0}^1 P(S_{i1} = j | \mathbf{a}) \log p_j + \\
& \sum_{i=1}^n \sum_{t=2}^T \sum_{k=0}^1 \sum_{j=0}^1 P(S_{it-1} = k, S_{it} = j | \mathbf{a}) \log p_{kj} + \\
& \sum_{i=1}^n \sum_{l=1}^L \sum_{t=1}^T \sum_{j=0}^1 P(S_{it} = j, b_i = r_l | \mathbf{a}) \delta_{it} \log P(a_{it} | S_{it} = j, b_i = r_l) + \\
& \sum_{i=1}^n \sum_{l=1}^L P(b_i = r_l | \mathbf{a}) \log \pi_l
\end{aligned} \tag{4}$$

2.2.3 Adapted forward-backward Algorithm

To account for the random effect in the emission distribution we use a modified version of the forward-backward algorithm that conditions on the discrete RE for person i [4]. The forward and backward quantities are calculated recursively as shown in equations 5 and 6. Thus we have the following quantities: $\alpha_{it}(j, r_l) = P(a_{i1}, \dots, a_{it}, S_{it} = j | b_i = r_l)$ and $\beta_{it}(j, r_l) = P(a_{it+1}, \dots, a_{iT} | S_{it} = j, b_i = r_l)$. We can then calculate the required quantities for equations 15 and 17 as shown by equations 8 and 9.

$$\alpha_{it}(j, r_l) = \begin{cases} p_j f(a_{i1} | S_{i1} = j, r_l) & \text{if } t = 1 \\ \sum_{k=0}^1 \alpha_{it-1}(k, b_l) p_{kj} P(a_{it} | S_{it} = j, b_i = r_l)^{\delta_{it}} & \text{if } t > 1 \end{cases} \tag{5}$$

$$\beta_{it}(j, r_l) = \begin{cases} \sum_{k=0}^1 p_{jk} P(a_{it+1} | S_{it+1} = k, b_i = r_l)^{\delta_{it}} \beta_{it+1}(k, r_l) & \text{if } t < n \\ 1 & \text{if } t = n \end{cases} \quad (6)$$

$$P(\mathbf{a}) = \prod_{i=1}^n \sum_{l=1}^L P(\mathbf{a} | b_i = r_l) P(b_i = r_l) = \prod_{i=1}^n \sum_{l=1}^L \sum_{j=0}^1 \alpha_{iT}(j, r_l) \pi_l \quad (7)$$

$$P(b_i = r_l | \mathbf{a}) = \frac{P(\mathbf{a} | b_i = r_l) P(b_i = r_l)}{P(\mathbf{a})} = \frac{\sum_{j=0}^1 \alpha_{iT}(j, r_l) \pi_l}{P(\mathbf{a})} \quad (8)$$

$$P(S_{it} = 0, b_i = r_l | \mathbf{a}) = \frac{P(S_{it} = 0, \mathbf{a} | b_i = r_l) P(b_i = r_l)}{P(\mathbf{a})} = \frac{\alpha_{it}(0, r_l) \beta_{it}(0, r_l) \pi_l}{P(\mathbf{a})} \quad (9)$$

$$P(S_{it} = 1 | \mathbf{a}) = \frac{\sum_{l=1}^L P(S_{it} = 1, \mathbf{a} | b_i = r_l) P(b_i = r_l)}{P(\mathbf{a})} = \frac{\sum_{l=1}^L \alpha_{it}(1, r_l) \beta_{it}(1, r_l) \pi_l}{P(\mathbf{a})} \quad (10)$$

$$\begin{aligned} P(S_{it-1} = k, S_{it} = j | \mathbf{a}) &= \frac{P(S_{it-1} = k, S_{it} = j, \mathbf{a})}{P(\mathbf{a})} \\ &= \frac{\sum_{l=1}^L \alpha_{it}(k, r_l) p_{kj} P(a_{it} | S_{it} = j, b_i = r_l) \beta_{it}(j, r_l) \pi_l}{P(\mathbf{a})} \end{aligned} \quad (11)$$

2.2.4 Parameter Estimates

To maximize each parameter, we take the derivative with respect to that parameter and set the derivative to 0. It is important to note the modular nature of this method as the initial, transition, emission, and mixing (π_l) probabilities can be maximized independently. Using the previously described adapted forward-backward algorithm, we can calculate equations 12-17, which give closed form solutions for the initial, emission, and mixing parameters. As we cannot observe μ_0 or r_l individually, we cannot estimate either independently. This does not pose an issue as the sum of the two quantities is the necessary component for the model and can be estimated. We will refer to ν_l as the cluster mean in future sections.

$$\hat{p}_j = \frac{\sum_{i=0}^n P(S_{i1} = 0|\mathbf{a})}{n} \quad (12)$$

$$\hat{\mu}_0 + \hat{r}_l = \hat{\nu}_l = \frac{\sum_{i=1}^n \sum_{t=1}^T a_{it} P(S_{it} = 0, b_i = r_l|\mathbf{a})}{\sum_{i=1}^n \sum_{t=1}^T P(S_{it} = 0, b_i = r_l|\mathbf{a})} \quad (13)$$

$$\hat{\sigma}_0^2 = \frac{\sum_{i=1}^n \sum_{l=1}^L \sum_{t=1}^T (a_{it} - \nu_l)^2 P(S_{it} = 0, b_i = r_l|\mathbf{a})}{\sum_{i=1}^n \sum_{l=1}^L \sum_{t=1}^T P(S_{it} = 0, b_i = r_l|\mathbf{a})} \quad (14)$$

$$\hat{\mu}_1 = \frac{\sum_{i=1}^n \sum_{t=1}^T a_{it} \delta_{it} P(S_{it} = 1|\mathbf{a})}{\sum_{i=1}^n \sum_{t=1}^T \delta_{it} P(S_{it} = 1|\mathbf{a})} \quad (15)$$

$$\hat{\sigma}_1^2 = \frac{\sum_{i=1}^n \sum_{l=1}^L \sum_{t=1}^T (a_{it} - \mu_1)^2 P(S_{it} = 1|\mathbf{a})}{\sum_{i=1}^n \sum_{l=1}^L \sum_{t=1}^T P(S_{it} = 1|\mathbf{a})} \quad (16)$$

$$\hat{\pi}_l = \sum_{i=1}^n \frac{P(b_i = r_l)}{n} \quad (17)$$

Unlike the previous parameters, no closed form solution for the transition probabilities exist. Instead, we preform a single Newton-Raphson step on the derivative of the likelihood at each iteration of the EM algorithm. Thus, $\beta_j^* = \beta_j - (\frac{\partial^2 \ell}{\partial \beta_j^2})^{-1} \frac{\partial \ell}{\partial \beta_j}$, where β_j is our current estimate and β_j^* is our updated estimate.

3 Simulation Study Results

As noted in the introduction, the goal of this paper is to supply guidelines for MHMM estimation. Namely, do MHMMs provide a substantial advantage compared to HMMs, and if so how many support points are necessary for the NPDE of the RE distribution. We have designed a simulation study to answer these questions.

For the simulation study, we first simulate the sequence of MC states corresponding to the wake/sleep state of person i at time t according to pre-specified initial and transition probabilities. We vary both the number of people (1000 and 5000) and the length of time per person (one day and one week of follow up). Then for each person we draw an individual level RE from its distribution H . We considered different underlying RE distribution such that H is normal, gamma, normal/gamma mixture, t with 2 degrees of freedom, and t with 3 degrees of freedom (figure 1). We then simulate the observed activity data where $a_{it} \sim N(2 + u_i, 3)$ if person i is awake at time t and $a_{it} \sim N(0, 2)$ if person i is asleep at time t . The parameters of the MHMM were estimated, where the number of support points was varied from 1 to 6.

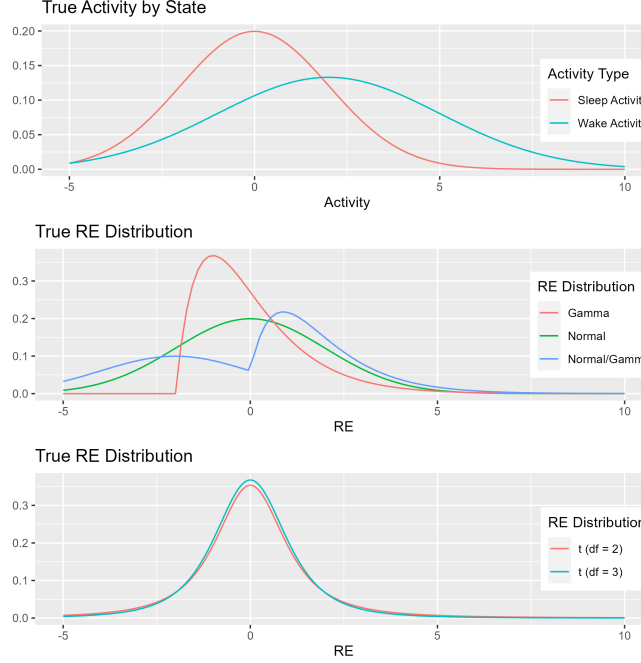


Figure 1: Distributions used in simulation study. Top plot shows wake (no RE) and sleep activity distribution. The bottom two plots show the different continuous RE distributions. RE distributions have been split up over two plots to increase readability.

Finally we use the Viterbi algorithm to construct the most likely sequence of wake/sleep states given our estimated parameters. We can then compare the estimated sequence with the true wake/sleep sequence. All of this was repeated 100 times for each combination (number of people, length of observation, choice of H).

The top plot of figure 1 shows the wake (without a RE) and sleep activity distribution. Each individual's wake activity distribution would be shifted to the right or left depending on if u_i is positive or negative. The bottom two plots show the different continuous RE distributions selected. The 5 choices for H have been split up into two plots to increase readability.

Figure 2 shows the results from the simulation. The y-axis for this figure is the percent agreement between the estimated wake/sleep sequence and the true wake sleep sequence. The color represents the number of support points, where the dark purple is one support point and the light green is 6. The x-axis represents the different simulation settings (days of follow up, number of participants, and RE distribution). Taking the left most purple point, we can follow the line down and see that the point represents the percent of the wake/sleep sequence correctly predicted when the simulated data had 1 day of follow up, 1000 participants, and the continuous RE comes from a gamma distribution.

As noted above, one support point is equivalent to leaving out the random effect, which in turn simplifies the mixed HMM to a standard HMM. As can be seen from figure 2, as the purple line is the lowest, one

Total Accuracy by Model, Sample Size, and RE Distribution

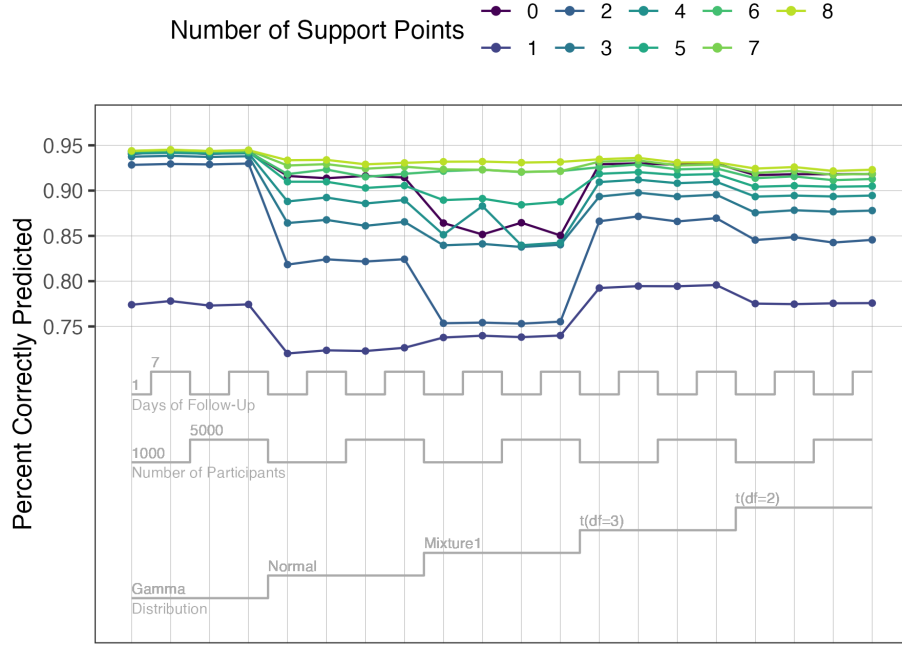


Figure 2: Nested loop plot of simulation results for total accuracy of predicted wake/sleep sequence. Each point is the median of 100 simulations and color indicates the number of support points. The X axis indicates the simulation settings, which are a combination of days follow-up, number of participants, and RE distribution.

support points has the lowest accuracy. This indicates that we see substantial accuracy gains from using a mixed HMM (with any number of support points) compared to a standard HMM when there truly is a RE in the emissions distribution. We see that this accuracy increase is true for all simulation settings, meaning that the MHMM is more accurate than the HMM for all combinations of sample size and underlying RE distribution.

Our next question was about the number of support points needed for the NPDE of the RE. We see that this is mainly dependent upon the underlying continuous RE distribution and not the sample size in most situations. When H is gamma, two support points suffice. When H is normal, three support points may be preferred to two, but the returns diminish quickly after that. When H is a gamma/normal mixture, four support points are needed. For the t distributions, sample size plays a minor role as well. For a t distribution with 3 degrees of freedom the trade off between computation time and number of support points needs to be evaluated as there are minimal, but present, differences for two, three, and four support points. For the 1 day of follow up with 5000 participants we see a large dip for two support points. This occurs because when the number of people increases, it is more likely that an extreme individual RE value is simulated. Thus one

of the support points is more likely to be placed to account for extreme values leaving only one support point to account for the remaining activity measurements. When increasing to a total of three support points, two can be used for the bulk and one for extreme values. A similar trend can be seen for a t distribution with two degrees of freedom, however, as the RE is even more spread out, more support points are necessary. A t distribution with two degrees of freedom may not be a realistic scenario, however figure 2 shows that with only 6 support points we can accurately predict the wake/sleep cycle under more extreme conditions.

To get a better understanding of how the method is working as a whole, we can look at metrics that are more specific than overall accuracy. Figure 3 shows the sensitivity (left column) and precision (right column) for the wake (top row) and sleep (bottom row) states. Recall that wake sensitivity is the percent of all truly wake states that we accurately predict as wake, and wake precision is the percent of predicted wake states that are truly wake (this may also be referred to as the positive predictive value). When we fit a standard HMM (one support point) we see that although the sleep sensitivity is high, the wake sensitivity is very low. This is because unless the activity for time t is very high, the state at time t is predicted to be sleep. Therefore we are classifying all low activity wake behavior as sleep. This can be seen by looking at the precision. The sleep precision is very low because we classify truly wake states as sleep. On the other hand, wake precision is very high because although we rarely predict wake, when we do we are most likely correct as we only predict wake if we see a high activity measure.

When the number of support points is increased, the wake sensitivity increases, while the sleep sensitivity decreases. This occurs as although we are better at classifying sedentary wake activity as wake, we also misclassify some sleep activity as wake. This causes wake precision to decrease and sleep precision to increase. Overall though, total accuracy is increased when the number of support points is increased as we can better classify wake states when we observe low activity measurements.

The number of support points needed depends on the spread of the underlying continuous RE distribution. When the spread is smaller, such as in the gamma simulation, two support points are sufficient. When the spread is larger, for instance as in the normal distribution, more support points are necessary. Looking closely at the 100 simulations for 5000 people with a week of follow up when H is the normal distribution we can get a better sense of how increasing the number of support points increases overall accuracy. This simulation corresponds to the eighth column of points starting from the left in figure 2.

Figure 4 contains information on the cluster mean ($\hat{\nu}_l$) in the top row and the mixing proportion (π_l) in the bottom row. Each gray box indicated the total number of support points used in the model and the column of the plot is the specific support points starting with the first on the left and the last. Each boxplot incorporates data from 100 simulations. With one support point we have one cluster at around 3.75 and roughly 67% accuracy. With two support points we still have a cluster at around 3.75 and an additional

Sensitivity and Precision by Model, Sample Size, and RE Distribution

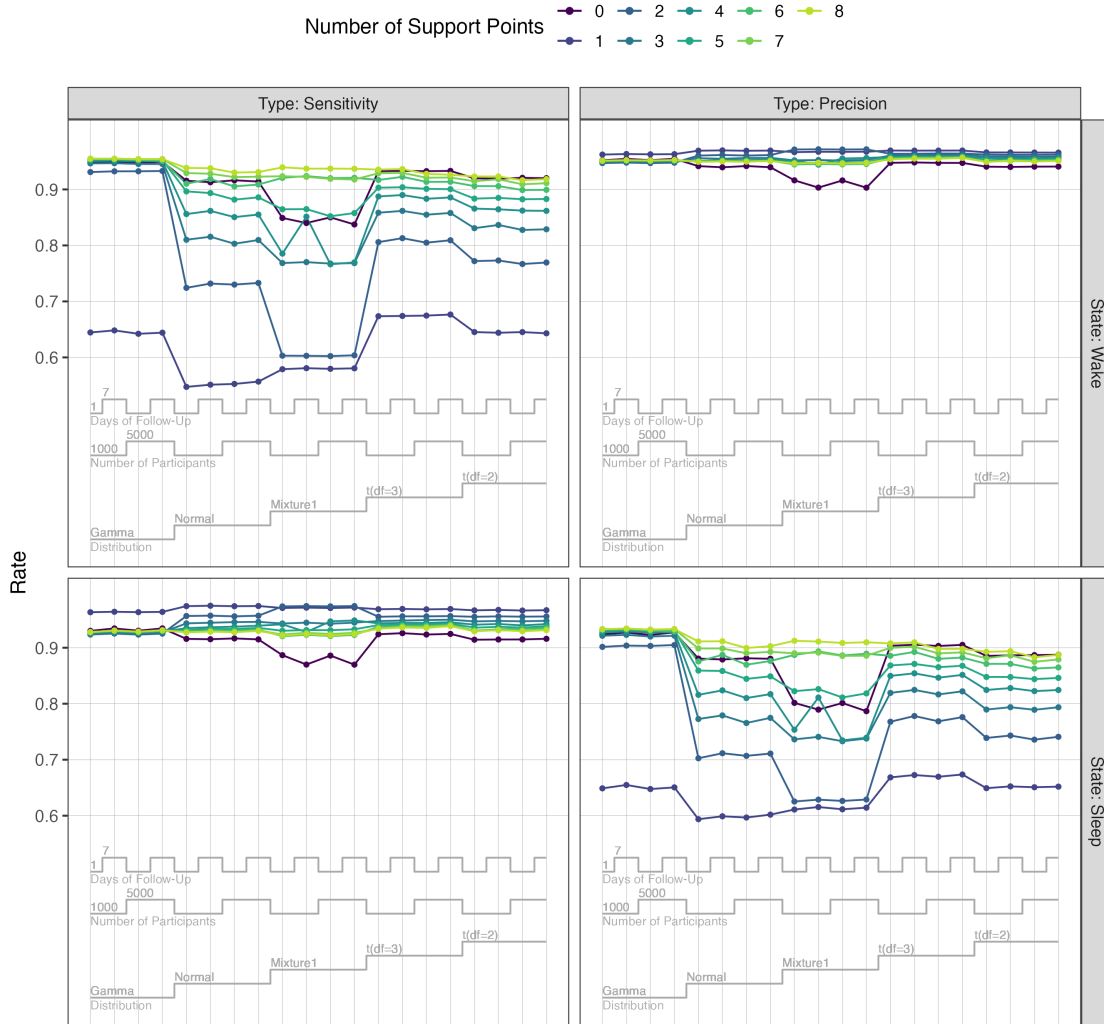


Figure 3: Nested loop plot of simulation results for sensitivity (left column) and precision (right column) for wake (top row) and sleep (bottom row). Each point is the median of 100 simulations and the color indicates the number of support points. The X axis indicates the simulation settings, which are a combination of days follow-up, number of participants, and RE distribution. Precision may also be referred to as the positive predictive value.

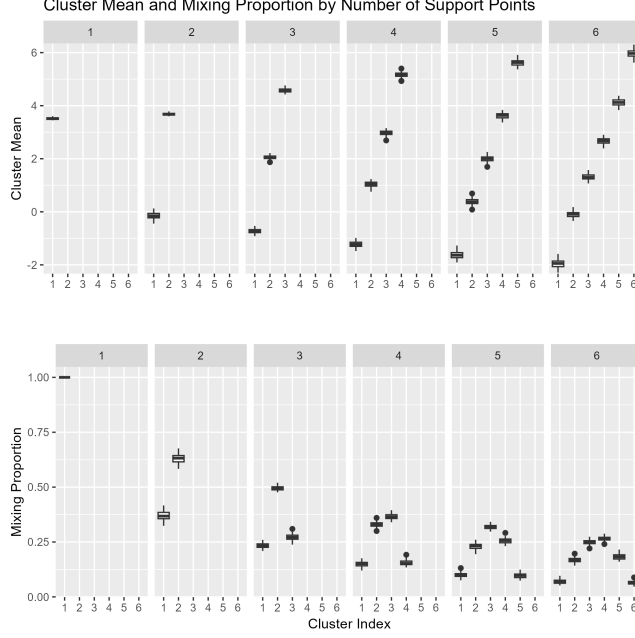


Figure 4: Cluster mean (top row) and mixing proportion (bottom row) for number of support points. Each column signifies the number of support points starting with one on the left and six on the right. Cluster mean represents $\nu_l = \mu_0 + r_l$ and the mixing proportion is r_l . Each boxplot uses data from 100 simulations.

cluster below 0. This new cluster around 0 is responsible for the ability to accurately predict the underlying state for sedentary people (i.e. those whose mean wake activity is similar to their sleep activity) and increases the overall accuracy to 75%. However with these two support points, we may still inaccurately predict the underlying state when we observe a mean activity between 0 and 3.75. For instance, if we observe a mean activity of 2 for person i , it is unclear which cluster person i belongs to. When we use three support points the clusters are now at -0.75 , 2 , and 4.5 and can accurately cover a wide range of mean wake activities.

As noted before, there is a trade-off between the number of support points and computation time that must be balanced. Increasing the number of support points increases the accuracy of the state reconstruction, however there are diminishing returns. As the necessary computation time roughly scales linearly with the number of support points, it is pertinent that we choose enough support points to accurately estimate the sequence without significant computational burden. Figure 5 is a nested loop plot showing the median running time in hours. We see that the increasing the number of support points generally increases the median running time. Additionally, for all of the simulations barring the t distribution with two degrees of freedom, two to four support points is sufficient for maximum accuracy as there is a steep drop off afterwards. For a t distribution with two degrees of freedom it may be beneficial to use six support points, despite the increased time.

Median Running Time by Model, Sample Size, and RE Distribution

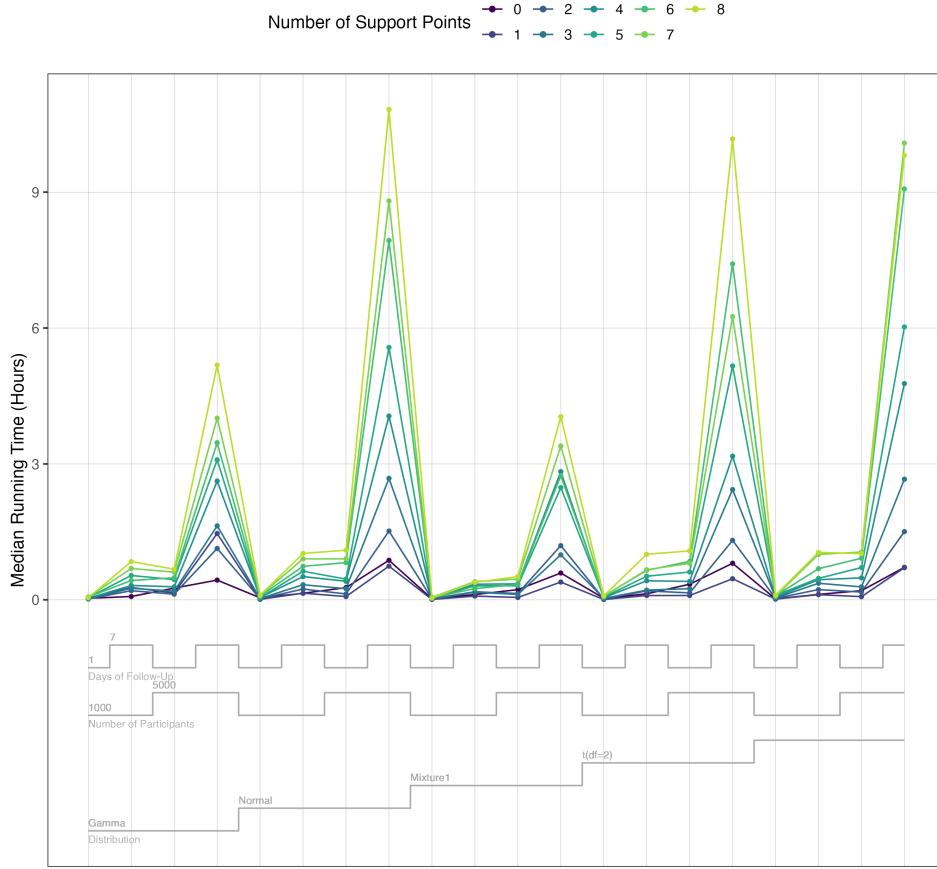


Figure 5: Nested loop plot of simulation results for median running time in hours. Each point is the median of 100 simulations and the color indicates the number of support points. The X axis indicates the simulation settings, which is a combination of days follow-up, number of participants, and RE distribution.

4 Conclusion

Mixed hidden Markov models are a recent adaptation of HMMs which can account for individual level heterogeneity. In this paper we have shown that when the data is truly generated with a RE in the emissions distribution, a MHMM preforms much better than a HMM for state prediction. As the RE distribution is estimated using nonparametric density estimation, we have also shown that only a small number of support points are needed, where the exact number depends on the underlying continuous RE distribution. When this distribution has a higher variance, more support points are necessary for accurate state estimation. Although increasing the number of support points increases overall accuracy, it also increases the time needed to fit the model. Therefore, a balance must be found between accuracy and computation time. We suggest using two to four support points, as this provides both high accuracy and shorter running times.

References

- [1] Rachel MacKay Altman. Mixed hidden markov models. *Journal of the American Statistical Association*, 102(477):201–210, 2007.
- [2] Alan Julian Izenman. Review papers: Recent developments in nonparametric density estimation. *Journal of the american statistical association*, 86(413):205–224, 1991.
- [3] Leonard E. Baum, Ted Petrie, George Soules, and Norman Weiss. A maximization technique occurring in the statistical analysis of probabilistic functions of markov chains. *The Annals of Mathematical Statistics*, 41(1):164–171, 1970.
- [4] Antonello Maruotti. Mixed hidden markov models for longitudinal data: An overview. *International Statistical Review / Revue Internationale de Statistique*, 79(3):427–454, 2011.